

Expanded View Figures

Figure EV1. Microarray and clustering analysis of Immortomouse™ clonal preadipocyte cell lines.

- A pH measurement of confluent preadipocyte cell lines with different adipogenic differentiation potential. The cells were scored on a scale from 1 to 4 for adipogenic differentiation after Oil Red O staining (1: < 25%; 2: 25–50%; 3: 50–75%, and 4: 75–100% of cells differentiated). Data are shown as mean \pm SEM of 4–10 cell lines/group.
- B Clonal preadipocyte cell lines used for microarray analysis. Cells were scored on a scale from 1 to 4 for adipogenic differentiation after Oil Red O staining (1: < 25%; 2: 25–50%; 3: 50–75%, and 4: 75–100% of cells differentiated) and 1–4 for media acidification by media color based on scale in Fig 2B (1: pH < 6.5; 2: pH from 6.5 to 6.9; 3: pH from 7.0 to 7.6; 4: pH > 7.7). Cells were selected for differentiation scores of 2 or greater and variable media acidification rates.
- C Affinity propagation clustering of preadipocyte clonal cell line gene expression. Exemplars are representatives of their cluster.
- D Hierarchical clustering utilizing the average method of agglomeration of preadipocyte clonal cell line gene expression.
- E Principal component analysis of preadipocyte clonal cell line gene expression.
- F Bright-field image of clonal preadipocyte lines after *in vitro* adipogenic, osteogenic, and chondrogenic differentiation. Adipocytes, osteocytes, and chondrocytes were stained with Oil Red O, Alizarin Red, and Alcian Blue, respectively. Original photographs were at 10 \times magnification (left panel). Scale bar = 100 μ m.

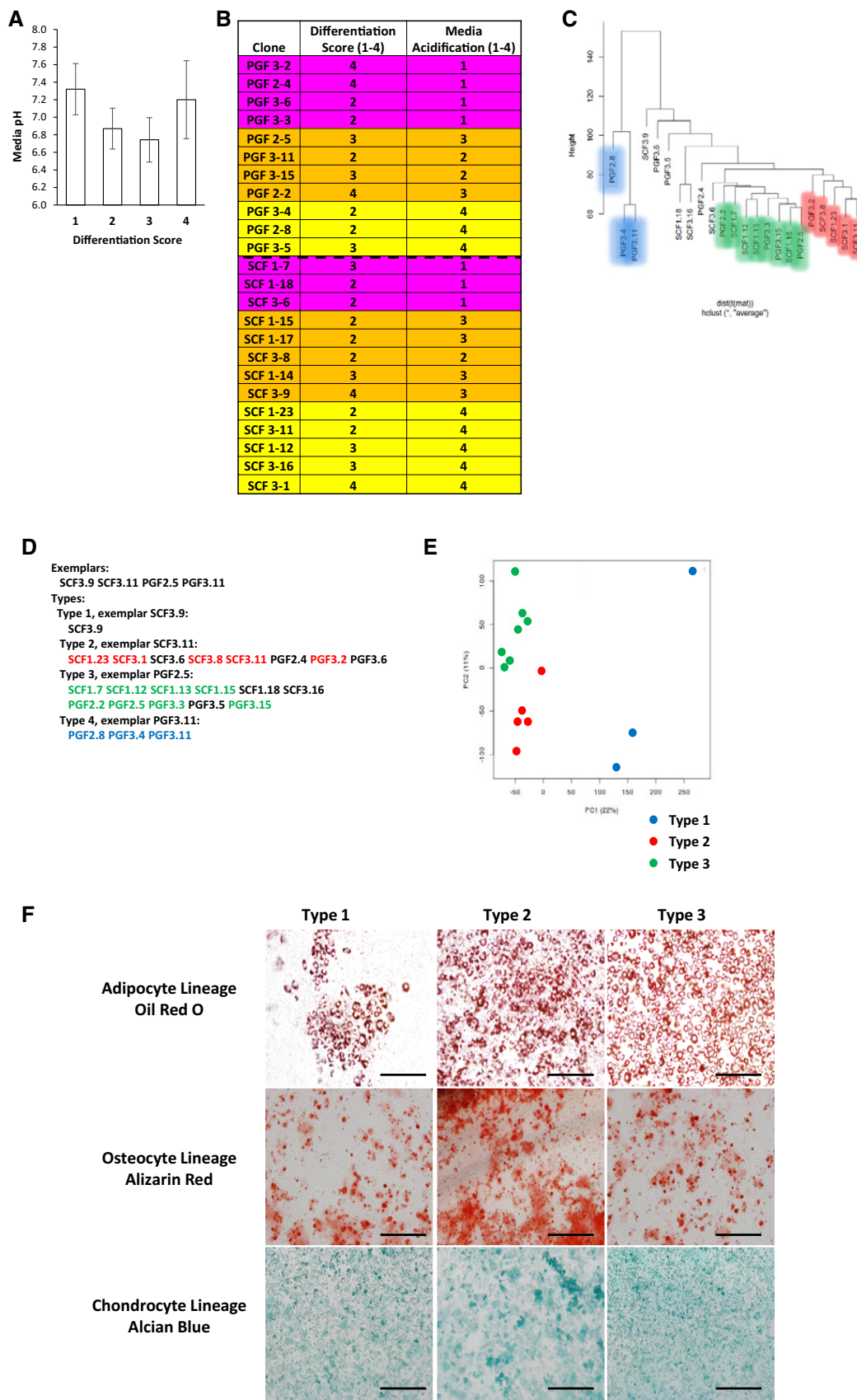


Figure EV1.

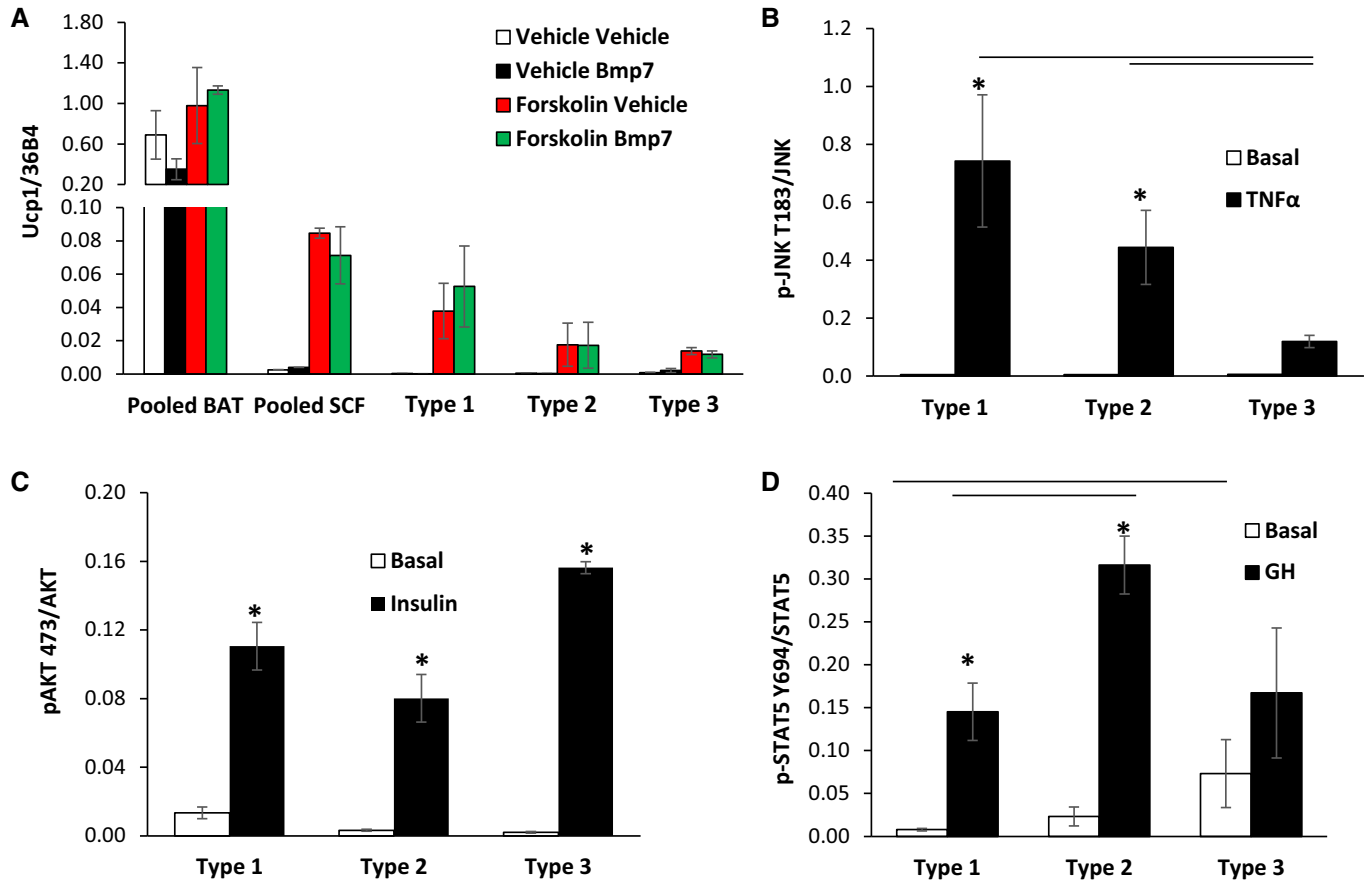


Figure EV2. Measurement of *Ucp1* expression and quantitation of signaling in preadipocyte cell cultures in response to exogenous stimuli.

A qPCR analysis for *Ucp1* in RNA isolated from Immortomouse adipocyte cell lines: pooled brown (BAT), pooled subcutaneous (SCF), Type 1, Type 2, and Type 3, after *in vitro* differentiation. Cells were treated \pm 3.3 nM BMP7 for 3 days prior to differentiation or treated \pm 10 μ M forskolin for 4 h. Data are shown as mean \pm SEM of 2–7 cell lines per group.

B–D Quantitation of Western blots depicted in Fig 4I. Data are shown as mean \pm SEM of three independent cell lines per group; each experiment was performed at least twice. Bars indicate significant differences between groups ($P < 0.05$; two-way ANOVA) in all panels. Asterisks indicate significant differences between basal and treated samples ($P < 0.05$; Student's *t*-test).

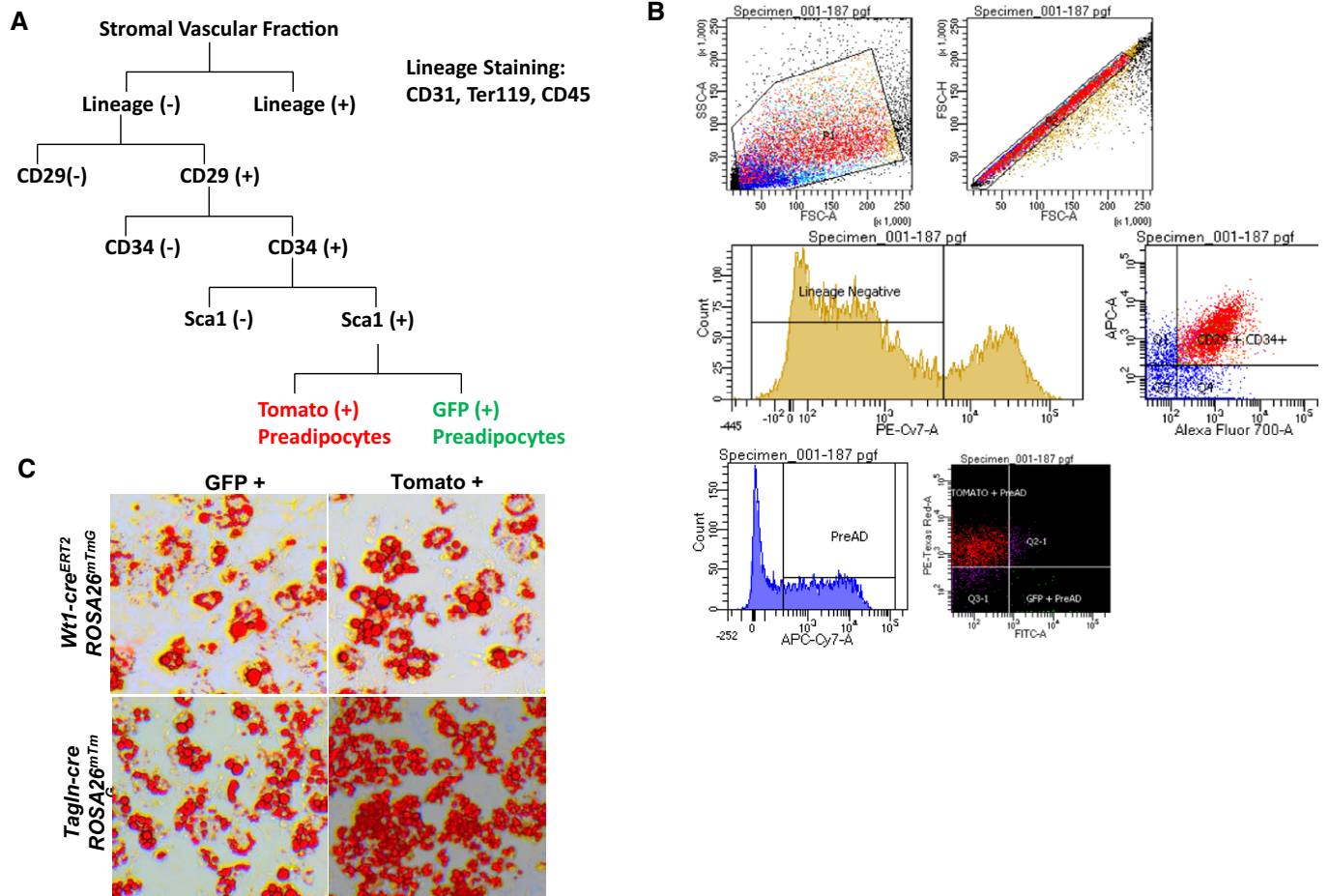


Figure EV3. FACS Sorting and Adipogenic Differentiation of Rosa26^{mT/mG} preadipocytes.

A Schematic of FACS sorting for GFP- and Tomato-positive preadipocytes.

B Representative FACS plot of LacZ (+) APCs from the subcutaneous and perigonadal fat depots of Tbx15-LacZ male mice at 6–8 weeks of age.

C Bright-field image of primary mGFP- and mTomato-positive preadipocytes after *in vitro* adipogenic differentiation. Neutral lipids were stained with Oil Red O, and original photographs were at 10× magnification (left panel).

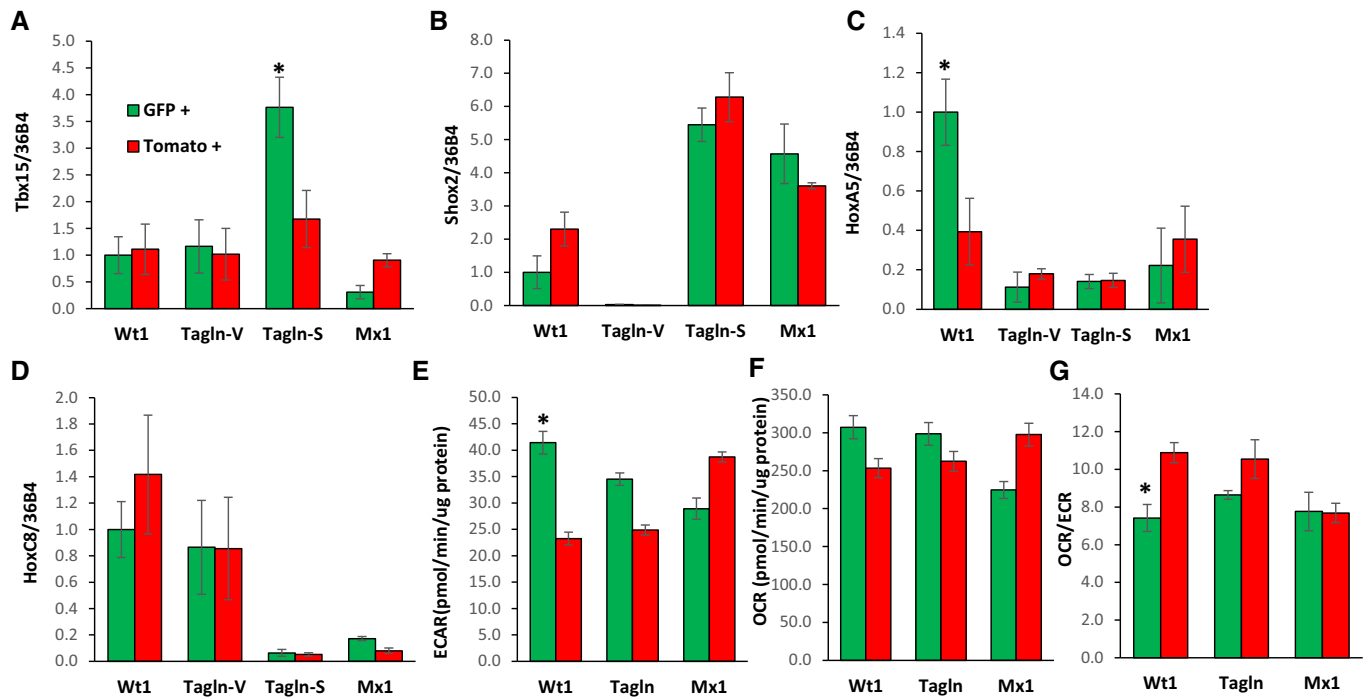


Figure EV4. Gene expression and maximal metabolic rates of primary preadipocyte subpopulations.

A–D Expression levels of *Shox2*, *Tbx15*, *HoxC8*, and *HoxC5* mRNA were compared using quantitative real-time PCR (qPCR) in primary preadipocytes isolated from white adipose tissue of 5- to 6-month-old Wt1-cre^{ERT2};Rosa26^{mT/mG}, Tagln-cre;Rosa26^{mT/mG}, and Mx1-cre;Rosa26^{mT/mG} male mice. mGFP- and mTomato-positive preadipocytes were isolated from the pooled visceral fat depots (perigonadal, perirenal, mesenteric, and pericardial) of Wt1-cre^{ERT2};Rosa26^{mT/mG} mice, the pooled subcutaneous fat depots (subcutaneous and scapular white) of Mx1-cre;Rosa26^{mT/mG}, and both the pooled visceral (Tagln-V) and subcutaneous depots (Tagln-S) from Tagln-cre;Rosa26^{mT/mG} mice. Data are shown as mean ± SEM of 4–6 mice/group.

E Maximal extracellular acidification rate (ECAR) of immortalized mGFP- and mTomato-positive preadipocytes was determined by calculating the area under the curve (AUC) during measurements of maximal extracellular acidification rate. The whole experiment was repeated twice. Data are shown as mean ± SEM of three cell lines per group.

F Maximal respiration of preadipocytes was of immortalized mGFP- and mTomato-positive preadipocytes determined by calculating the area under the curve (AUC) during measurements maximal of oxygen consumption rate (OCR). The whole experiment was repeated twice. Data are shown as mean ± SEM of three cell lines per group.

G Ratio of maximal oxygen consumption rate (OCR) to maximal extracellular acidification rate (ECAR) of immortalized mGFP- and mTomato-positive preadipocytes.

Data information: Asterisks indicate significant differences between mGFP- and corresponding mTomato-positive preadipocytes isolated from the same mouse line ($P < 0.05$; paired two-way ANOVA) in all panels. Bars indicate significant differences between mGFP preadipocytes isolated from different mice lines ($P < 0.05$; two-way ANOVA).

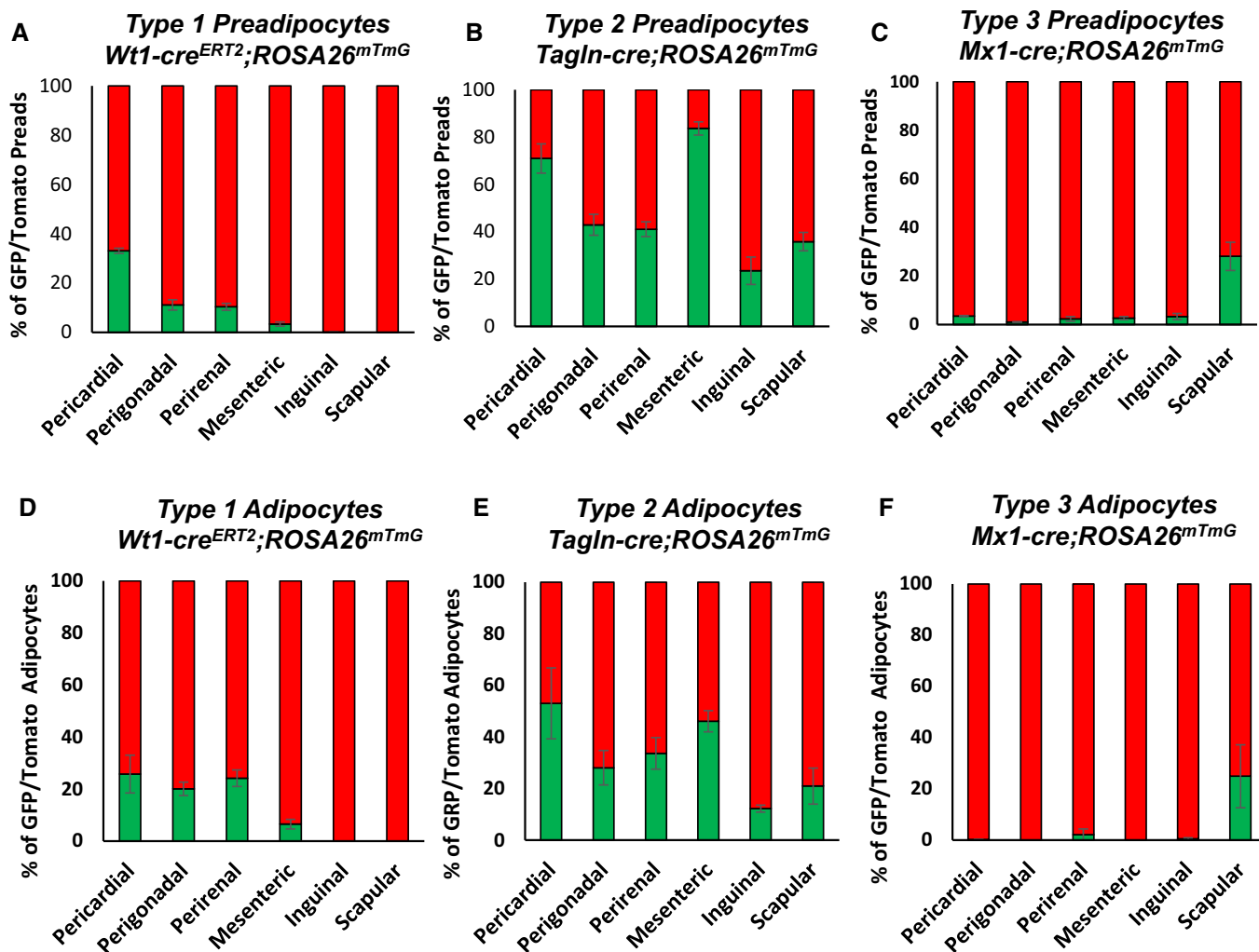


Figure EV5. Preadipocytes and adipocyte subpopulations in female mice.

A–C Number of mGFP- and mTomato-positive preadipocytes isolated by FACS from each of the indicated white adipose depots from 5- to 6-month-old female *Wt1-cre^{ERT2};Rosa26^{mT/mG}*, *Tagln-cre;Rosa26^{mT/mG}*, and *Mx1-cre;Rosa26^{mT/mG}* mice. Data are shown as mean ± SEM of 4–9 mice.

D–F Quantitation of mGFP- and mTomato-positive adipocytes from each of the indicated white adipose depots from 5- to 6-month-old female *Wt1-cre^{ERT2};Rosa26^{mT/mG}*, *Tagln-cre;Rosa26^{mT/mG}*, and *Mx1-cre;Rosa26^{mT/mG}* mice. Adipocytes were counted from four non-overlapping images/depot/mouse. Data are shown as mean ± SEM of 4–9 mice.